Allosteric Aptamers Controlling a Signal Amplification Cascade Allow Visual Detection of Molecules at Picomolar Concentrations†

Nickolas Chelyapov*

Laboratory for Molecular Science, University of Southern California, Los Angeles, California 90089, and California Institute of Molecular Medicine, Ventura, California 93003

Received October 15, 2005; Revised Manuscript Received December 29, 2005

ABSTRACT: A broadly applicable homogeneous detection system has been developed. It utilizes components of the blood coagulation cascade in the presence of polystyrene microspheres (MS) as a signal amplifier. Russell's viper venom factor X activator (RVV-X) triggers the cascade, which results in an eye-visible phase transition (precipitation) of MS bound to clotted fibrin. An allosteric RNA aptamer, RNA132, with affinity for RVV-X and human vascular endothelial growth factor ($VEGF_{165}$) was created. RNA132 inhibits enzymatic activity of RVV-X. The effector molecule, $VEGF_{165}$, reverses the inhibitory activity of RNA132 on RVV-X and restores its enzymatic activity, thus, triggering the cascade and enabling the phase transition. As few as 5 fmol of $VEGF_{165}$ could be detected by the naked eye within an hour. Similar results were obtained for another allosteric aptamer modulated by a protein tyrosine phosphatase. The assay is instrumentation-free for both processing and readout and can be modified to detect molecules to which aptamers can be obtained.

Detecting specific molecules is a crucial task for medicine, biotechnology, chemical and biodefense, and environmental protection. Many new detection systems are developed every year with increasing specificity and sensitivity. These systems include the latest developments in biotechnology and nanotechnology. All of them have one common feature: they employ sophisticated and expensive equipment for the processing and/or the readout of the results. This paper presents an approach for a broadly applicable detection system without using any instrumentation for both processing and readout.

In the last several years, aptamers have become widely used as sensors and diagnostic agents with a high level of specificity and sensitivity (*1*−*10*). Among other advantages, aptamers can be used in homogeneous assays, thus, eliminating reagent immobilization and reducing processing time and manipulation steps (*4*, *10*). Aptamers can acquire allosteric properties similar to enzymes (*8*, *11*−16), and therefore, they can be used for detecting "effector" molecules (*8*, *15*). To achieve the level of sensitivity that rivals more conventional immunoassays (*1*, *2*, *15*), aptamer-based detection systems also have to use sensitive and sophisticated instrumentation for processing and readout. To free the readout and the processing procedure from any kind of instrumentation, an approach is explored based on allosteric aptamers controlling the biochemical amplification cascade. The biochemical amplification cascade is based on the components of the blood coagulation cascade (BCC)[1] in the presence of polystyrene microspheres (MS). BCC-MS amplification cascade results in an eye-visible phase transition, that is, the precipitation of MS bound to the clotted fibrin. Controlled by an allosteric aptamer, the BCC-MS amplification cascade becomes the BCC-MS detection system.

EXPERIMENTAL PROCEDURES

Materials. All plasticware including 96-well plates (flat bottom) used in this study were nonstick or low-binding from Ambion and Corning. RNase-free water was from Ambion. Haematologic Technologies supplied the following reagents for the human blood coagulation cascade: Fibrinogen, Prothrombin, Factor Va, Factor X, snake venom protease RVV-X, and phospholipid vesicles (PCPS). SPECTROZYMEfXa (SPZXa) was from American Diagnostica. PCR and RT-PCR reagents and T7 RNA Polymerase kits were from Promega and Epicentre. Human $VEGF_{165}$, human $VEGF_{121}$, murine $VEGF_{165}$, zebrafish $VEGF_{165}$, endocrine gland VEGF, and human VEGF/P*l*GF heterodimer were from R&D Systems and USB. Polystyrene microspheres were from Bangs Laboratories. Ready-made polyacrylamide gels were from Invitrogen. Oligonucleotides were synthesized and purified by IDT or Qiagen.

All reactions took place in 50 mM imidazole-HCl and 3 mM $CaCl_2$ buffer, pH 7.8 (IC buffer). Snapshots of the 96-well plates were taken by a Memorex flatbed scanner, model 6142u.

BCC-MS Amplification Cascade. A typical reaction mix contained 600 nM PCPS, 230 nM Fibrinogen, 170 nM Prothrombin, 870 fM Factor Va, 580 pM Factor X, and a 1/450−1/350 dilution of polystyrene microspheres (10%

† This work was partially funded by grants from the National Science Foundation (CCF-0323749) and DARPA-ONR (N00014-98-1-0664).

* Correspondence information: phone, (213) 740-8491; fax, (213) 740-8631; e-mail, chelyapo@usc.edu.

[1] Abbreviations: BCC, blood coagulation cascade; MS, polystyrene microspheres; BCC-MS, blood coagulation cascade in the presence of polystyrene microspheres; PAGE, polyacrylamide gel electrophoresis; 40N, a 40-mer random nucleic acid sequence.

10.1021/bi052106i CCC: $33.50
Published on Web 01/27/2006

solids) 0.77−1.0 μm in diameter in IC buffer. One hundred microliters of the reaction mix was dispensed into the wells of a 96-well plate to which 5−10 μL of a test solution, for example, RVV-X, was added. After this, the plate was immediately placed into a microplate reader (Genios, Tecan) and shaken for 10−30 s prior to OD_{405} measurements at 5−10 min intervals. The relative effect (0 meaning no effect, and 1 meaning maximal effect) of $VEGF_{165}$ on the inhibition of the phase transition by RNA132 was calculated according to the following formula, which allowed graphic presentation for the dynamic range of the reaction:

$$(t_{1/2}^{+\text{RNA132/}-\text{VEGF165}} - t_{1/2}^{+\text{RNA132/}+\text{VEGF165}})/(t_{1/2}^{+\text{RNA132/}-\text{VEGF165}} - t_{1/2}^{-\text{RNA132/}+\text{VEGF165}})$$

where $t_{1/2}$ is the time for a 50% reduction in absorbance. The same formula was applied for the calculation of the relative effect for PTPase.

The BCC-MS reaction can be "frozen" at any stage by adding EDTA to a 10 mM final concentration.

SELEX Protocol and the Creation of Allosteric Aptamers. Sequences for the initial DNA template library (40N) and primers for the SELEX for aptamer to RVV-X were taken from ref *17*. Large-scale PCR amplification and all other subsequent synthetic and selection steps were performed as described in refs *17*−*19* without modification. The initial selection involved 500 pmol of random RNA library (3×10^{14} molecules). After each round of selection, RNA was tested in a nitrocellulose filter binding assay to determine the dissociation constant of aptamer−protein complexes (K_d) (*19*) and in a single point binding assay with equimolar concentrations of protein and RNA (50 nM) (*20*). In the latter experiments, one set of filters was washed with IC buffer. Another set of filters was washed with IC buffer and 300 mM NaCl (high salt buffer) to remove more of the nonspecifically bound RNA. After the fifth and ninth round of selection, RNA was reverse-transcribed; DNA was amplified by PCR and cloned. Each time, 45 clones were sequenced to determine the presence of consensus sequences. Cloning and sequencing were performed by Laragen.

Three $VEGF_{165}$-binding RNA aptamers, 12t, 84t, and 100t, described in ref *21*, and three other $VEGF_{165}$-binding RNA aptamers, VPt2, VPt22, and VTt44, described in ref *22*, were synthesized using unmodified NTPs and tested in a gel-shift assay with $VEGF_{165}$. Aptamer VTt44 showed the highest affinity for $VEGF_{165}$ in the IC buffer (data not shown), since it was initially selected in the presence of calcium, which was absolutely required for high-affinity binding of this aptamer to $VEGF_{165}$ (*22*). Please note that Ca ions are essential for BCC-MS amplification cascade.

Allosteric aptamers were created either by directly fusing the 5′-end of RNA37s with the 3′-end of an effector aptamer or by inserting an effector aptamer RNA a number of bases downstream into the RNA37s.

RVV-X Activity Determination with SPECTROZYMEfXa (RVV-X-SPZXa Assay). SPECTROZYMEfXa is a chromogenic substrate for the activated Factor X. RVV-X by itself (10 μL, 1.7 nM) or pretreated with aptamers (17 nM) was incubated with Factor X (170 nM) and mixed with 140 μL of SPECTROZYMEfXa (5 mM, IC buffer). Appearance of the chromophore, *p*-nitroanilide acetate, was monitored over time at 405 nm in a microplate reader. The final measurement was taken 10 min after the onset of the reaction. The inhibitory effect of an aptamer on the RVV-X activity was calculated according to the following formula:

$$[1 - (A^{\text{RVV}-\text{X}+\text{RNA}} - A^{\text{RNA}})/(A^{\text{RVV}-\text{X}} - A^{\text{RNA}})] \times 100\%$$

RNA Folding and Minimum Free-Energy Calculations. Predictions of the RNA folding patterns with or without pseudoknots and calculations of minimum free energy (ΔG) were done according to algorithms and software presented in refs *23* and *24*. Visual representation of the RNA secondary structure based on the above predictions was done using PseudoViewer2 software (*25*).

DNA Competition Assay for Mapping of RNA132 Binding Sites for RVV-X and $VEGF_{165}$. DNA molecules complementary to various segments of RNA132 were synthesized (see the list in Table 1) and used as competitors to RVV-X and $VEGF_{165}$ in binding to ^{32}P-labeled RNA132. The complexes were analyzed in a gel-shift assay utilizing 6% PAGE (0.5× TBE). RNA132 (100 fmol) was annealed with DNA (200 fmol) by incubating the mix at 70 °C for 1 min with slow cooling to room temperature. Proteins were added to the complex at room temperature, and after 15 min of incubation, the samples were subjected to PAGE. Volumes for bands, determined by Phosphorimager "Storm" (Molecular Dynamics), corresponding to RNA132 complexes with RVV-X or $VEGF_{165}$, with no competing DNA added, were taken as 100% binding. When a full-length DNA complement (DNA I) was competing with the proteins for binding to RNA132, no bands corresponding to the RNA−protein complexes were detected for either of the proteins; thus, binding for them was 0%. In a control experiment, proteins were annealed with the DNA used at 10-fold higher concentrations. No binding was detected between competing DNA and the proteins.

RESULTS

Homogeneous BCC-MS Amplification Cascade. A biochemical signal amplification cascade, utilizing components of the BCC cascade in the presence of MS was described as a part of a heterogeneous ELISA assay (*26*). The BCC portion of the amplification cascade consisted of Factors X, Va, II (Prothrombin), and I (Fibrinogen). BCC was triggered by a specific metalloproteinase, the Russell's viper venom factor X activator (RVV-X) (*27*). RVV-X-initiated BCC resulted in an eye-visible phase transition, that is, precipitation of MS bound to the clotted fibrin. The assay showed sensitivity of 10−100 fg/mL for RVV-X, which corresponds to 10−100 zmol of the protein detected in 100 μL of a test solution in 60 min. The disadvantages of the above assay include its basis on a standard solid-support ELISA format that requires multiple washes and reagent transfers. Furthermore, the above assay relies on several specific, not readily available reagents, one of which is a monoclonal antibody conjugated to RVV-X (*26*).

In the present study, an effective approach overcoming these issues is proposed. An allosteric aptamer would substitute for antibodies and conjugates and would render the assay homogeneous, eliminating washing and minimizing reagent transfer steps. An allosteric aptamer will bind to RVV-X and inhibit its enzymatic activity, while subsequent

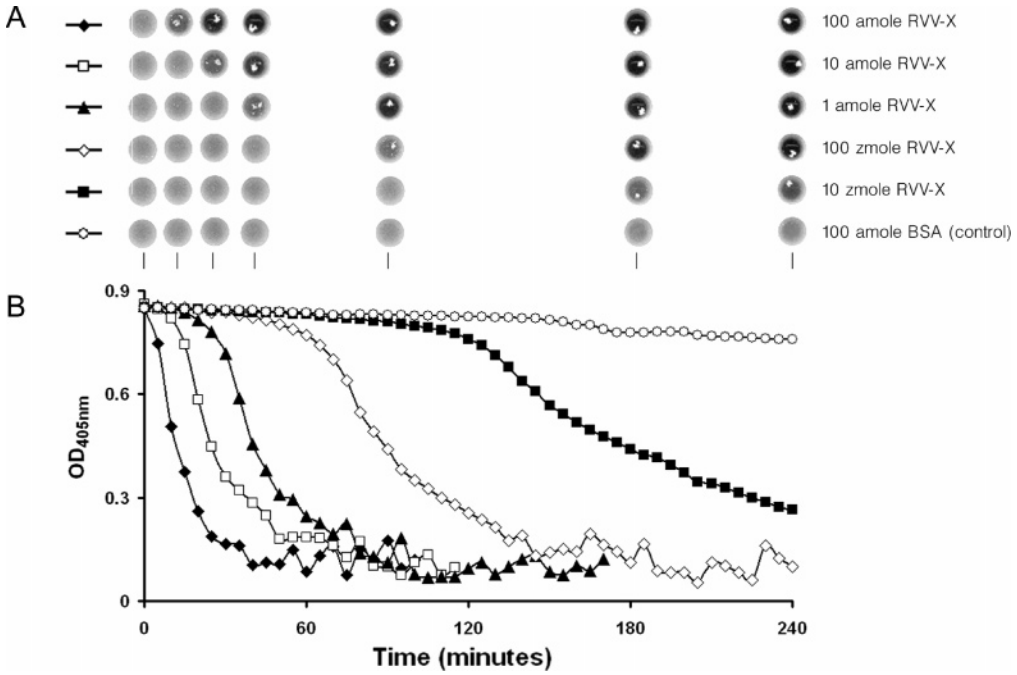

FIGURE 1: Kinetics of the phase transition (precipitation of MS bound to the clotted fibrin) in the BCC-MS amplification cascade triggered by the different concentrations of RVV-X. (A) Visual presentation of the 96-well plate obtained on a flatbed scanner at the time of 50% reduction in absorbance ($t_{1/2}$) for a given concentration of RVV-X. (B) Optical density at 405 nm measured on a microplate reader in the same wells at 5-min intervals.

binding of an effector molecule to the aptamer will modulate the inhibitory effect by reversing it. Thus, an on/off switch for the RVV-X activity will be created depending on the presence of an effector molecule. The allosteric aptamer-controlled detection system based on BCC in the presence of MS (BCC-MS) will require only one variable component, a part of the allosteric aptamer specific to the effector molecule.

Components for the homogeneous BCC-MS amplification cascade were derived from refs *26* and *28*. Modifications, suggested by Dr. G. Doellgast (personal communication), included substitution of the Factor V with the Factor Va and substitution of the rabbit brain cephalin with the commercially available phospholipid vesicles. Figure 1 shows the kinetics of the phase transition (clot formation) caused by the RVV-X activity in the BCC-MS amplification cascade monitored both visually and spectrophotometrically at 405 nm. Snapshots of the wells taken at the time of 50% reduction in absorbance ($t_{1/2}$) for different RVV-X concentrations show distinct differences among the wells depending on the progress of the phase transition (Figure 1A). At the beginning (time zero), all wells have a uniformly whitish, milky appearance, as the MS are in suspension. The well with no RVV-X added (open circles) remains the same during the entire course of the experiment. After 12 min, corresponding to $t_{1/2}$ for 100 amol of RVV-X (solid diamonds), less opaque material is seen in the corresponding well. No changes are observed in the other wells at this time. At 26 min, corresponding to $t_{1/2}$ for 10 amol of RVV-X (open squares), less opaque material is seen in the well, as was at 12 min for the well with 100 amol of RVV-X. The MS in the well with the 100 amol of RVV-X are coagulated by this time, and the well has a clear black background. This coagulation pattern is repeated in subsequent wells. Thus, the homogeneous BCC-MS amplification cascade is adequate for the detection of small quantities of RVV-X by the naked eye.

Selection of an Aptamer to RVV-X. An RNA aptamer binding to RVV-X was obtained via standard SELEX protocol (*17*−*19*). The progress of the selection was monitored by determining the dissociation constant of the RNA−protein complex (K_d) and by determining the fraction of RNA that binds to the target protein at the same "high" concentration (50 nM) of both the aptamer and the target protein in a single point binding assay. The latter assay was performed using both the binding buffer and the high-salt buffer (binding buffer and 300 nM NaCl) to decrease the input of nonspecifically bound complexes (*20*). The initial pool of unselected RNA (RNA0) had a K_d value of 550 ± 23 nM. In a single point binding assay, 6.3% of RNA0 preincubated with RVV-X was bound to the filter when the binding buffer was used for washing, and 2.2% of the RNA0 stayed bound to the filter when the high-salt buffer was used for washing, with 1.2% of background noise. After the ninth round of selection, the K_d for RNA9 decreased to 2.2 ± 1.9 nM, and the results for the single point binding assay were 55% and 43%, respectively, with 2% background noise. A consensus sequence (RNA9c) was derived from the analysis of 45 clones of RT-PCRed RNA9.

The full-length RNA9c (87 bases) containing the consensus 40-mer sequence flanked by the primers showed a 43% inhibitory effect on the RVV-X enzymatic activity in the RVV-X-SPZXa assay. A systematic deletion mutagenesis applied to RNA9c enabled the isolation of a minimal 43-mer RNA37s (Figure 2A) with 84% inhibitory effect on RVV-X in the RVV-X-SPZXa assay. RNA37s also showed a concentration-dependent inhibitory effect on the RVV-X-induced clot formation in the BCC-MS detection system (Figure 3A). Binding of RNA37s to RVV-X was confirmed in a gel-shift experiment (Figure 4A).

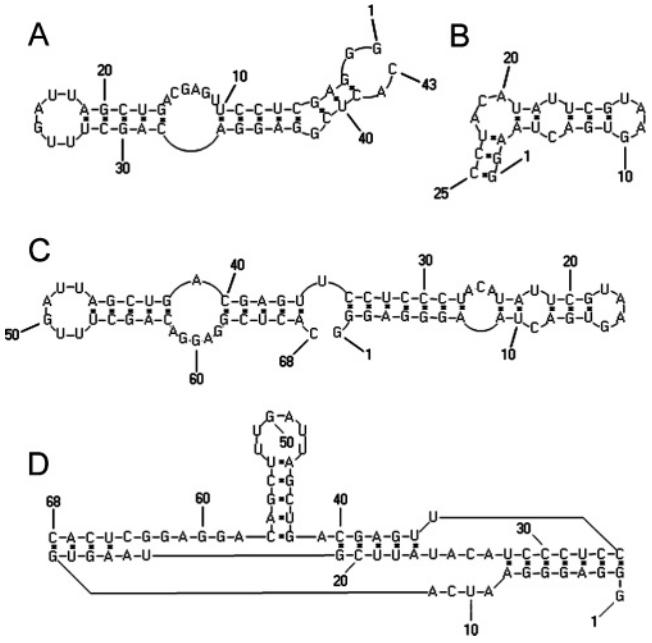

FIGURE 2: Schematic representation of the secondary structure folding for the RNA aptamers. (A) RNA37s; (B) VTt44(−2); (C) RNA132 without pseudoknots; (D) RNA132 with pseudoknots.

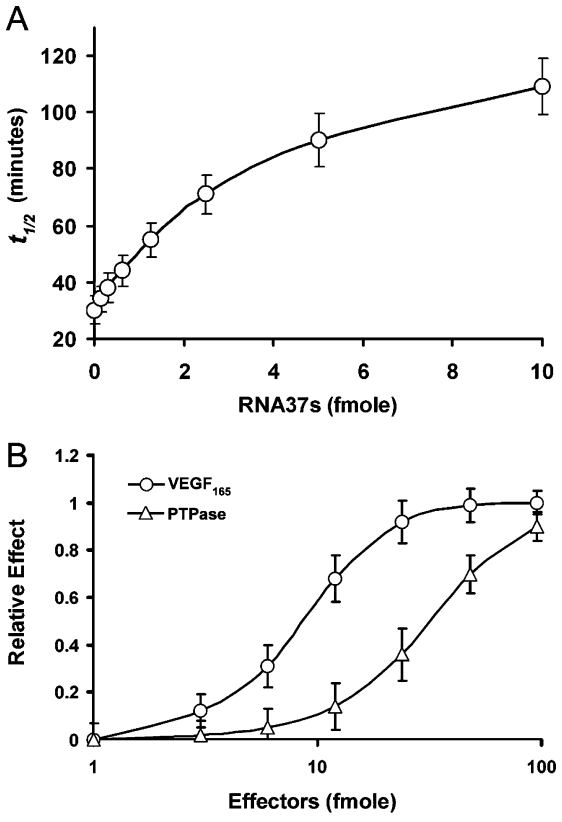

FIGURE 3: Kinetics of the phase transition in the BCC-MS detection system. (A) In the presence of different concentrations of RNA37s. (B) The reversal of the inhibitory effect of RNA132 on the phase transition by different concentrations of human $VEGF_{165}$ and PTPase. The relative effect was calculated according to the formula in the Experimental Procedures.

Construction of an Allosteric Aptamer. Human $VEGF_{165}$ was chosen as an effector molecule for the construction of an allosteric aptamer. The choice of $VEGF_{165}$ was based on several criteria, including the availability of high-affinity aptamers to $VEGF_{165}$ (*21*, *22*), one of which was shown to be an efficient anti-$VEGF_{165}$ agent in vivo (*29*). Also there are several natural analogues of the human $VEGF_{165}$ that can be adequate controls for the specificity of the detection system, and there are commercially available highly sensitive ELISA assays for this protein that can serve as reference standards.

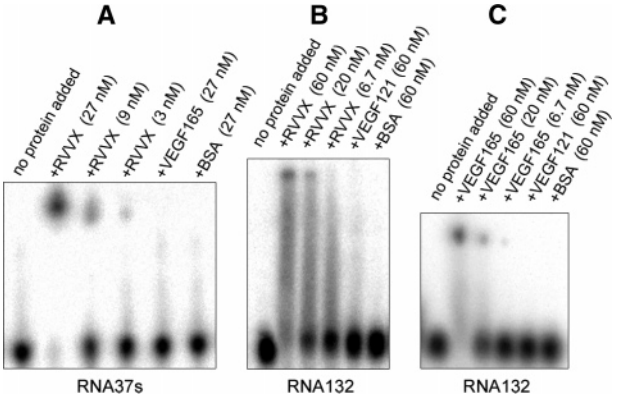

FIGURE 4: Gel-shift analysis of RVV-X and human $VEGF_{165}$ binding to RNA37s and RNA132.

An aptamer binding to $VEGF_{165}$, RNA ligand VTt44 (*22*), with one base omitted from both 5′- and 3′-ends, VTt44(−2), (Figure 2B), was inserted into RNA37s five bases downstream from its 5′-end to create the allosteric aptamer RNA132 (Figure 2C). This structure appeared to be more stable when compared with the "head-to-tail" version, where the 5′-end of RNA37s was directly fused with the 3′-end of VTt44(−2) ($\Delta G = -24.0$ kcal/mol versus $\Delta G = -18.0$ kcal/mol) (*23*, *24*). Presumably, putative RNA binding domains stayed accessible for both proteins in the chimeric RNA132. A possible conformation including pseudoknots was also predicted for RNA132 with $\Delta G = -27.0$ kcal/mol (Figure 2D) (*23*).

In a gel-shift assay, RVV-X and $VEGF_{165}$ were shown to bind to RNA132 at about equal concentrations (Figure 4B,C). The dissociation constants for both proteins, 5.7 ± 2.9 nM, appeared to be identical within experimental error. RNA132 was also tested in the RVV-X-SPZXa assay and showed 86% inhibitory effect, similar to the effect of RNA37s within experimental error. As tested in the BCC-MS detection system, the concentration-dependent inhibitory effect of RNA132 on the phase transition was also similar to RNA37s within experimental error.

The Effector Molecule, $VEGF_{165}$, Reverses Inhibition of the Phase Transition Caused by RNA132. As was shown in the RNA132-controlled BCC-MS detection system, $VEGF_{165}$ reversed the inhibitory effect of RNA132 on the RVV-X-triggered phase transition in a concentration-dependent mode (Figure 3B). This effect suggests a competition between $VEGF_{165}$ and RVV-X for binding to RNA132. The dynamic range for the effect of $VEGF_{165}$ on the reversal of the phase transition in the RNA132-controlled BCC-MS detection system appeared to be narrow, that is, about a 10-fold range of $VEGF_{165}$ concentrations (3−30 fmol). This was shown to be typical for the BCC-based detection systems (*28*). The sensitivity of the detection of $VEGF_{165}$ in the RNA132-controlled BCC-MS detection system is within the lower half of the linear range for the $VEGF_{165}$ concentrations detected by commercial ELISA assays.

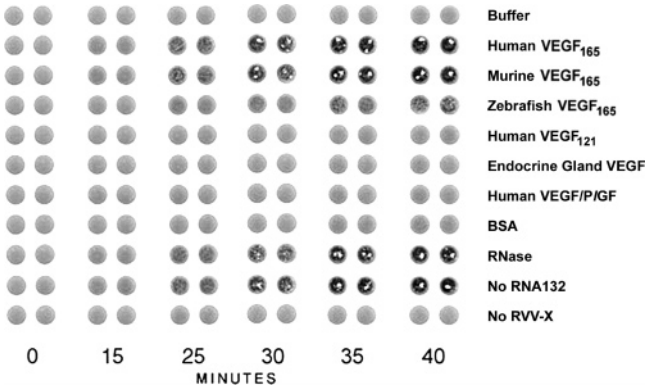

FIGURE 5: Visual presentation of the kinetics of clot formation in the RNA132-controlled BCC-MS detection system in the presence of 10 fmol of different proteins, except for 100 amol of RNase. Proteins were incubated with a mixture of RVV-X and RNA132 for 15 min at room temperature in 5−10 μL of IC buffer, followed by the addition of the components of the BCC-MS detection system. At the indicated time points, wells of the 96-well plate were scanned on a flatbed scanner. The results are presented in duplicates.

Another allosteric aptamer (RNA37sN71) modulated by a different effector molecule was created by fusing RNA37s with an aptamer to a protein tyrosine phosphatase (PTPase) from *Yersinia enterocolitica*, N71 (*30*). In the RNA37sN71-controlled BCC-MS detection system, the PTPase also reversed the inhibitory effect of RNA37sN71 on the RVV-X-triggered phase transition in a concentration-dependent mode (Figure 3B), although the curve describing the relative effect of the PTPase was shifted to higher concentrations of PTPase as compared with $VEGF_{165}$.

Specificity of the BCC-MS Detection System. Figure 5 presents the data on the specificity of the RNA132-controlled BCC-MS detection system for human $VEGF_{165}$. Human $VEGF_{165}$, murine $VEGF_{165}$, and zebrafish $VEGF_{165}$ have the same biological function and contain 165 of amino acids. Murine $VEGF_{165}$ has an 89% identity with human $VEGF_{165}$, where 147 of 165 amino acids are identical. Zebrafish $VEGF_{165}$ has about a 62% amino acid sequence identity with human $VEGF_{165}$. Human $VEGF_{121}$ is a truncated version of human $VEGF_{165}$, with 44 amino acids truncated downstream from position 110 of the polypeptide chain. Thus cysteine 137 of $VEGF_{165}$ that forms a photoinducible cross-link to a uridine at position 14 of RNA VTt44 (*22*) (which corresponds to position 13 of RNA VTt44(−2) and position 18 of RNA132) is missing in $VEGF_{121}$. Human VEGF/P*l*GF heterodimer is a protein artificially dimerized in vitro. It consists of human $VEGF_{165}$ and Placental growth factor. The amino acid sequence of endocrine gland VEGF is unrelated to that of human VEGF. The kinetics of the clot formation were similar in the wells containing human $VEGF_{165}$ and murine $VEGF_{165}$. In both cases, the coagulation process was complete within 40 min. This was not surprising, since human and murine $VEGF_{165}$ are highly homologous. At the same time point (40 min) when the wells containing human $VEGF_{165}$ demonstrated completed coagulation, the wells containing zebrafish $VEGF_{165}$ demonstrated the onset of coagulation. This can be explained by less homology (62%) between human $VEGF_{165}$ and zebrafish $VEGF_{165}$. Meanwhile, in the wells containing human $VEGF_{121}$, endocrine gland VEGF, human VEGF/PlGF, and BSA, phase transition has not been observed by that time. The results in Figure 5 clearly demonstrate the high specificity of the detection system.

Table 1: Mapping of RNA132 Binding Sites for RVV-X and VEGF165 in a DNA Competition Assay

DNA	base position number	percent binding	
		RVV-X	$VEGF_{165}$
none added	N/A[a]	100	100
I	1−68	0	0
II	31−68	10	48
III	36−68	17	64
IV	1−30	19	14
V	6−30	28	36
VI	8−28	51	42

[a] N/A, not applicable.

Exploration of the Possible Mechanism of the Allosteric Effect. An attempt was made to find a mechanism underlying the competition between $VEGF_{165}$ and RVV-X for the interaction with RNA132. DNA molecules complementary to different segments of RNA132 were used in the competition binding experiments of RVV-X and $VEGF_{165}$ to RNA132 (see Table 1). When a full-length DNA complement to RNA132 (DNAI) was used, no binding was observed for either of the proteins. When DNAII and DNAIII compete for the RVV-X binding to the 37s domain of RNA132, predictable low levels of RVV-X binding were detected. Annealing of DNAIV to the VTt44 domain of RNA132 significantly decreases $VEGF_{165}$ binding to RNA132. When shorter DNA fragments corresponding to the VTt44 domain of RNA132 (DNAV and DNAVI) were used for the competition, the impact of competing DNA on $VEGF_{165}$ affinity for RNA132 is decreased. An unexpected inhibitory effect of DNAIV and DNAV on RVV-X binding to RNA132 was also observed. A possible explanation is that the putative stem located between positions 2−8 and 28−34 in RNA132 (Figure 2C) is involved in the binding of both proteins. This can result in direct steric competition between the proteins. One can also speculate that the decrease of RVV-X binding in the presence of DNAIV and DNAV can be explained by assuming an alternative folding of RNA132 into a structure containing pseudoknots (Figure 2D). Further theoretical and experimental analyses re required to more clearly describe the molecular interactions resulting in allosteric properties of RNA132.

DISCUSSION

In this study, an allosteric RNA aptamer-based competitive homogeneous detection system with readout by the naked eye was achieved. This became possible by coupling an allosteric RNA aptamer with the biochemical signal amplification cascade, BCC-MS. The signal amplification cascade results in an eye-visible phase transition, that is, formation of the precipitate of polystyrene microspheres bound to clotted fibrin. The allosteric aptamer contains a domain that binds to RVV-X thus inhibiting BCC. There is another domain on the allosteric aptamer which binds to an effector molecule reversing the effect of the first domain. The latter domain of the aptamer is the only variable part of the detection system. Therefore, adjusting the detection system to a new effector molecule will involve only one molecular component, an aptamer to the effector molecule. Further, the detection system requires only two pipetting cycles compared

with 10 in the case of ELISA, and it requires less than an hour for its completion, compared with 4.5 h for ELISA. Most importantly, the naked eye is used as a readout instrument instead of expensive and rarely available equipment. These features make the detection system a good candidate as a platform for fieldable detection systems and make it competitive with ELISA.

ACKNOWLEDGMENT

The author thanks Syed Z. Salahuddin for providing the opportunity to carry out final experiments at the California Institute of Molecular Medicine; Jay Hesselberth for help with SELEX; and George Doellgast, Robert Dirks, Ravi Braich, Dustin Reishus, and Pablo Moisset de Espanes for helpful discussions.

REFERENCES

1. Osborne, S. E., Matsumura, I., and Ellington, A. D. (1997) Aptamers as therapeutic and diagnostic reagents: problems and prospects, *Curr. Opin. Chem. Biol. 1*, 5−9.
2. Jayasena, S. D. (1999) Aptamers: an emerging class of molecules that rival antibodies in diagnostics, *Clin. Chem. 45*, 1628−1650.
3. Brody, E. N., and Gold, L. (2000) Aptamers as therapeutic and diagnostic agents, *Mol. Biotechnol. 74*, 5−13.
4. Jhaveri, S. D., Kirby, R., Conrad, R., Maglott, E. J., Bowser, M., Kennedy, R. T., Glick, G., and Ellington, A. D. (2000) Designed signaling aptamers that transduce molecular recognition to changes in fluorescent intensity, *J. Am. Chem. Soc. 122*, 2469−2473.
5. Jhaveri, S., Rajendran, M., and Ellington, A. D. (2000) In vitro selection of signaling aptamers, *Nat. Biotechnol. 18*, 1293−1297.
6. Hamaguchi, N., Ellington, A., and Stanton, M. (2001) Aptamer beacons for direct detection of proteins, *Anal. Biochem. 294*, 126−131.
7. Silverman, S. K. (2003) Rube Goldberg goes (ribo)nuclear? Molecular switches and sensors made of RNA, *RNA 9*, 377−383.
8. Stojanovic, M. N., and Kolpashchikov, D. M. (2004) Modular aptameric sensors, *J. Am. Chem. Soc. 126*, 9266−9270.
9. Wang, X.-L., Li, F., Su, Y.-H., Sun, X, Li, X.-B., Schluesener, H. J., Tang, F., and Xu, S.-Q. (2004) Ultrasensitive detection of protein using an aptamer-based exonuclease protection assay, *Anal. Chem. 76*, 5605−5610.
10. Tombelli, S., Minunni, M., and Mascini, M. (2005) Analytical applications of aptamers, *Biosens. Bioelectron. 20*, 2424−2434.
11. Soukup, G. A. (2004) Aptamers meet allostery, *Chem. Biol. 11*, 1031−1032.
12. Wu, L., and Curran, J. F. (1999) An allosteric synthetic DNA, *Nucleic Acid Res. 27*, 1512−1516.
13. Vuyisich, M., and Beal, P. A. (2002) Controlling protein activity with ligand- regulated RNA aptamers, *Chem. Biol. 9*, 907−913.
14. Buskirk, A. R., Landrigan, A., and Liu, D. R. (2004) Engineering a ligand-dependent RNA transcriptional activator, *Chem. Biol. 11*, 1157−1163.
15. Nutiu, R., and Li, Y. (2004) Structure-switching signaling aptamers: transducing molecular recognition into fluorescence signaling, *Chem.−Eur. J. 10*, 1868−1876.
16. Cong, X., and Nielsen-Hamilton, M. (2005) Allosteric aptamers: targeted reversibly attenuated probes, *Biochemistry 44*, 7945−7954.
17. Fitzwater, T., and Polisky, B. (1996) A SELEX primer, *Methods Enzymol. 267*, 275−301.
18. Pollard, J., Bell, S. D., and Ellington, A. D. (2000) Design, synthesis, and amplification of DNA pools for in vitro selection, in *Current Protocols in Nucleic Acid Chemistry*, pp 9.2.1−9.2−23, Wiley, New York.
19. Jhaveri, S. D, and Ellington, A. D. (2000) In vitro selection of RNA aptamers to a protein target by filter immobilization, in *Current Protocols in Nucleic Acid Chemistry*, pp 9.3.1−9.3.25, Wiley, New York.
20. Cox, J. C., Hayhurst, A., Hesselberth, J., Bayer, T. S., Georgiou, G., and Ellington, A. D. (2002) Automated selection of aptamers against protein targets translated in vitro: from gene to aptamer, *Nucleic Acid Res. 30*, e108, 1−14.
21. Jelinek, D., Green, L. S., Bell, C., and Janjic, N. (1994) Inhibition of receptor binding by high-affinity RNA ligands to vascular endothelial growth factor, *Biochemistry 33*, 10450−10456.
22. Ruckman, J., Green, L. S., Beeson, J., Waugh, S., Gilette, W. L., Henninger, D. D., Claesson-Welsh, L., and Janjic, N. (1998) 2′-Fluoropyrimidine RNA-based aptamers to the 165-amino acid form of vascular endothelial growth factor ($VEGF_{165}$), *J. Biol. Chem. 273*, 20556−20567.
23. Dirks, R. M., and Pierce, N. A. (2003) A partition function algorithm for nucleic acid secondary structure including pseudoknots, *J. Comput. Chem. 24*, 1664−1677.
24. Dirks, R. M., and Pierce, N. A (2004) An algorithm for computing nucleic acid base pairing probabilities including pseudoknots, *J. Comput. Chem. 25*, 1295−1304.
25. Han, K., and Byun, Y. (2003) PseudoViewer2: visualization of RNA pseudoknots of any type, *Nucleic Acid Res. 31*, 3432−3440.
26. Strachan, N. J. C., and Ogden, I. D. (2000) A sensitive microsphere coagulation ELISA for *Escherichia coli* O157:H7 using Russell's viper venom, *FEMS Microbiol. Lett. 186*, 79−84.
27. Gowda, D. C., Jackson, C. M., Hensley, P., and Davidson, E. A. (1994) Factor X activating glycoprotein of Russell's viper venom. Polypeptide composition and characterization of the carbohydrate moieties, *J. Biol. Chem. 269*, 10644−10650.
28. Doellgast, G. J., Triscott, M. X., Beard, G. A., Bottoms, J. D., Cheng, T., Roh, B. H., Roman, M. G., Hall, P. A., and Brown, J. E. (1993) Sensitive enzyme-linked immunosorbent assay for detection of *Clostridium botulinum* neurotoxins A, B, and E using signal amplification via enzyme-linked coagulation assay, *J. Clin. Microbiol. 31*, 2402−2409.
29. Fish, G., Haller, J. A., Ho, A. C., Klein, M., Loewenstein, J., Martin, D., Orth, D., Rosen, R. B., Sanislo, S., Schwartz, S. D., et al. (2003) Anti-vascular endothelial growth factor therapy for subfoveal choroidal neovascularization secondary to age related macular degeneration. Phase II study results, *Ophthalmology 110*, 979−986.
30. Dell, S. D., Denu, J. M., Dixon, J. E., and Ellington, A. D. (1998) RNA molecules that bind to and inhibit the active site of tyrosine phosphatase, *J. Biol. Chem. 273*, 14309−14314.

BI052106I